



THE UNIVERSITY *of* EDINBURGH

Edinburgh Research Explorer

Seeing Through Solvent Effects using Molecular Balances

Citation for published version:

Mati, IK, Adam, C & Cockroft, S 2013, 'Seeing Through Solvent Effects using Molecular Balances' *Chemical Science*, pp. 3965-3972. DOI: 10.1039/C3SC51764K

Digital Object Identifier (DOI):

[10.1039/C3SC51764K](https://doi.org/10.1039/C3SC51764K)

Link:

[Link to publication record in Edinburgh Research Explorer](#)

Document Version:

Peer reviewed version

Published In:

Chemical Science

Publisher Rights Statement:

Copyright © 2013 by the Royal Society of Chemistry. All rights reserved.

General rights

Copyright for the publications made accessible via the Edinburgh Research Explorer is retained by the author(s) and / or other copyright owners and it is a condition of accessing these publications that users recognise and abide by the legal requirements associated with these rights.

Take down policy

The University of Edinburgh has made every reasonable effort to ensure that Edinburgh Research Explorer content complies with UK legislation. If you believe that the public display of this file breaches copyright please contact openaccess@ed.ac.uk providing details, and we will remove access to the work immediately and investigate your claim.



Post-print of a peer-reviewed article published by the Royal Society of Chemistry.
Published article available at: <http://dx.doi.org/10.1039/C3SC51764K>

Cite as:

Mati, I. K., Adam, C., & Cockroft, S. (2013). Seeing Through Solvent Effects using Molecular Balances. *Chemical Science*, 2013, 4, 3965-3972.

Manuscript received: 24/06/2013; Accepted: 22/07/2013; Article published: 23/07/2013

Seeing Through Solvent Effects using Molecular Balances^{**‡}

Ioulia K. Mati, Catherine Adam and Scott L. Cockroft*

EaStCHEM, School of Chemistry, Joseph Black Building, University of Edinburgh, West Mains Road, Edinburgh, EH9 3JJ, UK.

[*]Corresponding author; e-mail: scott.cockroft@ed.ac.uk, tel: +44 (0)131 650 4758

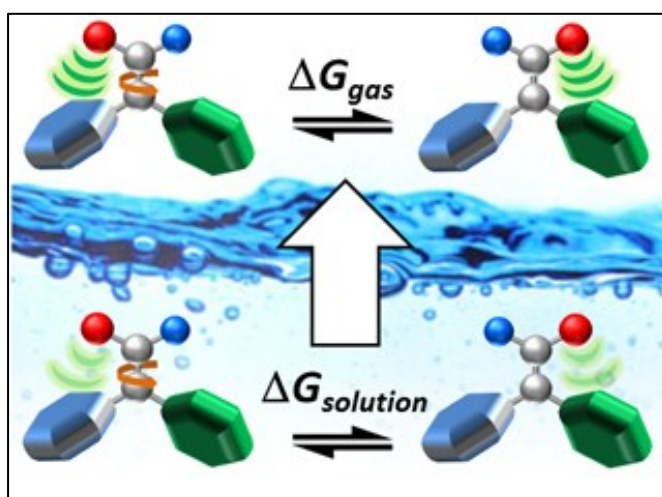
[**]We thank the School of Chemistry and Pfizer Ltd for funding PhD studentships for IKM and CA respectively.

[‡]Celebrating 300 years of Chemistry at Edinburgh.

Supporting information:

Electronic supplementary information (ESI) available: Additional data, and experimental and computational methods. See <http://dx.doi.org/10.1039/C3SC51764K>

Graphical abstract:



Summary:

A simple solvent model enables dissection of solvent effects to reveal the pseudo-gas-phase behaviour of molecular balances.

Abstract

The study of molecular interactions is often complicated by solvent effects. Here we have used a series of 11 synthetic molecular balances to measure solvent and substituent effects on the positions of conformational equilibria in 13 different solvents. Despite the simplicity of the model system, surprisingly complicated behaviour was seen to emerge from the interplay of conformational, intramolecular and solvent effects. Nonetheless, 138 experimental conformational free energies were analysed using a simple solvent model, which was able to account for both the major and more unusual patterns observed. The success of the solvent model can be attributed to its ability to facilitate consideration of individual intramolecular and solute-solvent interactions, as confirmed by comparison with NMR chemical shifts and DFT calculations. The approach provides a means of dissecting electrostatic and solvent effects to reveal pseudo gas-phase behaviour from experimental data obtained in solution. For example, the method facilitated the identification of an unexpected, but highly favourable $\text{C}=\text{O}\cdots\text{NO}_2$ interaction worth up to 3.6 kJ mol^{-1} , which was shown not to be driven by solvent effects.

Introduction

Non-covalent interactions underpin chemistry and biology. They determine the stereochemical outcomes of reactions,¹⁻³ ligand-receptor binding,⁴⁻⁷ and the structure and function of proteins, nucleic acids^{8,9} and other supramolecular architectures.^{10,11} However, few experimental approaches exist for dissecting individual contributions to the complicated arrays of interactions and solvent effects governing molecular behaviour.¹²⁻¹⁷

Molecular balances, pioneered by Ōki,¹⁸ and Wilcox,^{19,20} are a useful platform for the study of non-covalent interactions since the positions of conformational equilibria are determined by intramolecular interactions and solvent effects.²¹ Such systems have been used to measure a whole range of interactions including aromatic interactions,¹⁵⁻³¹ orthogonal dipolar interactions,³²⁻³⁴ and deuterium isotope effects.³⁵ Molecular balances present a number of advantages for the study of molecular recognition phenomena. Firstly, the geometries of intramolecular interactions are typically better defined than in supramolecular complexes. Secondly, they enable the measurement of very weak non-covalent interactions since conformational equilibria are sensitive to small free energy differences, while the intramolecular approach evades the significant entropic costs associated with bimolecular complexation.^{36,37} Finally, where variation of the solvent often adversely affects solubility and binding constants in supramolecular complexes, thermodynamic data can be extracted from molecular balances in any solvent provided that it is sufficiently soluble for an NMR spectrum to be obtained.

Even though molecular balances are inherently suited to the systematic study of solvent effects, they have rarely been used to examine more than a handful of solvents.^{15-17, 23-25} Here we have employed a series of simple molecular balances as a quantitative probe of electronic effects on the position of conformational equilibria in a wide range of solvents (Figures 1 and 2). Rotation about the formyl C–N bond in these balances was measured as 75.1 kJ mol⁻¹ (Fig. S21), which means that these balances exist in equilibrium between spectroscopically-distinct conformers on the NMR timescale. Since the chemical shift of the fluorine atom in the balances is sensitive to the rotational isomerisation of the formyl group, ¹⁹F-NMR was used to determine the conformational equilibrium constants (*K*) in a range of readily accessible solvents. 138 conformational free energy differences were determined for 11 molecular balances in 13 different solvents (using $\Delta G = -RT\ln K$). Despite the apparent simplicity of these balances, complicated behaviour was revealed as the substituents and solvents were varied (Table 1 and Figure 2).

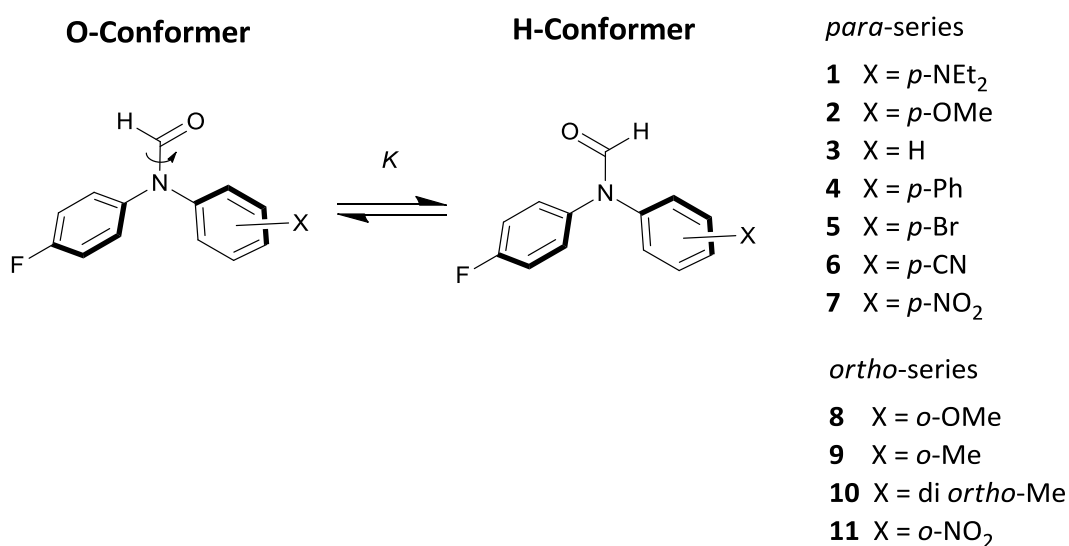


Figure 1. Conformational equilibrium for the formamide balances synthesised in this study.

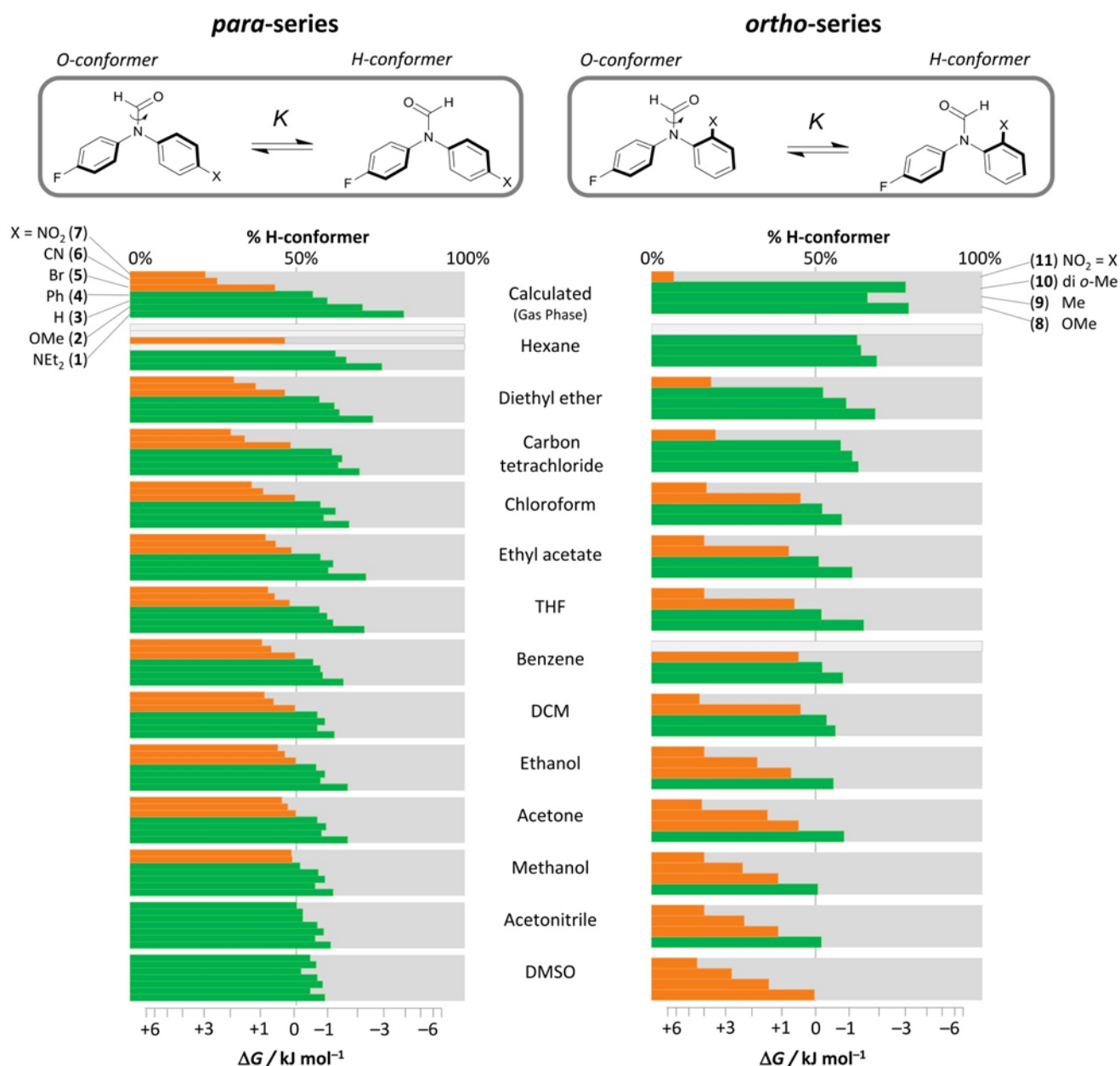


Figure 2. Percentages of H conformers and conformational free energies of balances **1** to **11** determined in 13 solvents and calculated by B3LYP/6-31G* in the gas-phase. Orange bars indicate positive ΔG values (O-conformer preferred) and green bars indicate negative ΔG values (H-conformer preferred). The missing values in hexane indicated by the light grey bars correspond to points where the balances were insufficiently soluble to obtain data, while the missing data for balance **11** in benzene was due to peak overlap in the NMR spectrum. Tabulated data are provided in Table S1 and also indicate whether deuterated or non-deuterated solvents were used.

Thus, these data were analysed using a simple solvation model to see whether it could provide any insight into the individual interactions in governing the observed behaviour.

Results and discussion

Conformational equilibrium constants were measured in the 13 solvents shown in Figure 2 and calculated in the gas-phase using B3LYP/6-31G* (Table S1). The major trends in the conformational energies of the *para*-substituted balances indicate that the equilibrium is driven by electronic substituent effects in apolar solvents, with the formyl oxygen preferring to lie over the least electron-rich ring. Accordingly, the balances generally follow the same pattern of energies; balances bearing X substituents that are more electron donating than fluorine (**1**, **2**, **3**, **4**, X = NEt₂ to Ph) prefer the H-conformer ($\Delta G < 0$), while balances with electron-withdrawing groups (**5**, **6**, **7**, X = Br, CN, NO₂) prefer the O-conformer ($\Delta G > 0$). The larger the electronic difference between the F-substituted and the X-substituted ring, the greater the magnitude of ΔG . The sensitivity of each balance to the electronic effects of the substituents is also highly dependent on the solvent. Apolar solvents have the largest conformational free energy differences, and are most similar to the calculated gas-phase energies (e.g. $\Delta G_{\text{exp}} = -2.4$ and $+2.0$ kJ mol⁻¹ for X = NEt₂ and NO₂, respectively in diethyl ether). As the solvents become more polar the energies digress further from the calculated gas-phase free energy and become closer to zero (e.g. -0.8 and -0.4 kJ mol⁻¹ for X = NEt₂ and NO₂ in DMSO).

While the major patterns in the *para*-substituted balances are easily rationalised, not all of the trends are so easily explained, particularly for the *ortho*-substituted balances (Figure 2, right column):

- i) The *para*-substituted balances bearing electron-withdrawing groups prefer the H-conformer as solvent polarity increases, which cannot be explained by gas-phase electrostatic effects. In the *ortho*-substituted balances the trend is reversed and the preference for the O-conformer increases with solvent polarity.
- ii) The *ortho*-Me, di *ortho*-Me and *ortho*-OMe balances are more sensitive to solvent effects than any of the *para*-substituted balances (including those bearing polar substituents such as NO₂ and CN).
- iii) The *ortho*-NO₂ balance is relatively insensitive to the modulating effects of the solvent and has the most extreme ΔG values ranging between $+3.5$ to $+4.5$ kJ mol⁻¹. This contrasts with the behaviour of the other *ortho*-substituted balances and the *para*-NO₂ balance, which are very sensitive to solvent effects.

In spite of the simplicity of the model system, it is difficult to rationalise these patterns without further analysis, other than to say that intramolecular electrostatic and solvent effects must both play a role in determining the conformational preferences. Thus, the challenge arises as to whether it is possible to dissect-out the individual factors contributing to the observed conformational free energies.

Dissecting solvent effects using a simple solvent model

Hunter's α/β hydrogen-bond model has been shown to account for¹⁵ and predict¹⁶ solvent effects on the conformational free energies of Wilcox molecular torsion balances, in addition to edge-to-face aromatic interactions in supramolecular complexes¹⁶ and hydrogen-bonding interactions in many different solvents and solvent mixtures.^{13,38} Thus, we were curious to ascertain whether a simple α/β solvation model would be able to account for the large volume of data obtained in the present study (comprising 138 experimental free energy measurements obtained for 11 different molecular balances in 13 solvents).

We reasoned that the conformational free energies would be governed by the intramolecular electrostatic and steric differences between the O- and the H-conformers (encoded by ΔE), and the global differences in the hydrogen-bond donor and acceptor constants of each conformer ($\Delta\alpha$ and $\Delta\beta$), as represented in Figure 3. This schematic representation only shows single hydrogen-bond donor and acceptor sites, but in reality the $\Delta\alpha$ and $\Delta\beta$ terms will be determined by the Boltzmann average of all possible solvation sites on each balance.

The experimental conformational free energies of each balance as the α_s and β_s hydrogen-bond donor and acceptor constants were varied (by changing the solvent) were fitted to the equation shown in Figure 3 using a least squares linear regression. Overall, the fitting gave an $R^2 = 0.96$ between the predicted ($\Delta G_{\alpha/\beta \text{ model}}$) and the experimental free energies (ΔG_{exp}) for all balances and solvents examined (Figure 4).³⁹ Notably, this fitting included all of the initially surprising results summarised in points i) to iii) above, but nonetheless, these ΔG values were as well predicted as the balances with the more easily rationalised conformational preferences.

The fitting process provides values of ΔE , $\Delta\alpha$ and $\Delta\beta$ for each of the balances examined, which provide insight into the individual interactions contributing to the experimental conformational free energies (Table 1). The high-quality correlation between the determined ΔE values and gas-phase conformational free energy differences calculated using B3LYP/6-31G* (ΔG_{DFT} , Figures 5a, Figures S5-11 and Table S5), confirm that the ΔE term corresponds to the intramolecular contributions to ΔG_{exp} . Notably, simply averaging the ΔG_{exp} values for each balance across all solvents examined resulted in a comparatively poorer correlation against ΔG_{DFT} , particularly for the *ortho*-substituted balances, which highlights the advantage of the energetic dissection facilitated by the α/β solvation model (Figure S3a). Consistent with a dominant electrostatic component, balances bearing electron-donating groups have negative ΔE , while those with electron-withdrawing substituents have positive ΔE values. The electrostatic component of ΔE is revealed in the correlations with both σ_m Hammett substituent constants (Figure 5b), and electrostatic potentials taken over the corresponding carbon atoms positioned *meta* to X substituents in the *para*-substituent series of balances (ESP_{meta}, Figure 5c).

Although high correlation coefficients are also seen in correlations of ΔG_{exp} values averaged across all solvents for the *para*-substituted balances, these graphs have significantly shallower gradients than those shown in Figures 5b-c (Figure S3b-c). The differences in the gradients arise because the damping effects of the solvent are simply averaged in the ΔG_{ave} plots shown in Figure S3, while the greater variation of the ΔE values (obtained by application of the α/β -model) is consistent with solvent effects being dissected away to reveal the pseudo-gas-phase behaviour resulting from intramolecular interactions. Overall, Figure 5 shows that the ΔE term follows the expected intrinsic stability trends (without the influence of solvent).

In contrast to the solvent-independent ΔE values, the energetic effects of $\Delta\alpha$ and $\Delta\beta$ are modulated by the solvent (via the $\beta_s\Delta\alpha$ and $\alpha_s\Delta\beta$ terms, as shown in Figure 3). In general, more polar solvents with larger α_s and β_s constants decrease ΔG differences between conformers because the sign of the $\Delta\alpha$ and $\Delta\beta$ terms oppose that of the ΔE term. The $\Delta\beta$ term varies more than $\Delta\alpha$ across the series of balances examined, and is consistent with solvation of the highly polar formyl oxygen atom having a large influence on the position of the conformational equilibrium (see electrostatic surface potentials in Figures S5-S11).

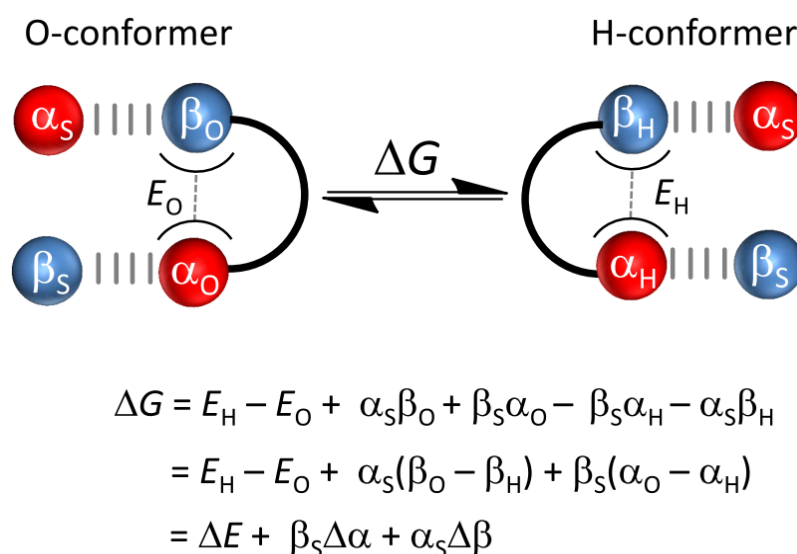


Figure 3. A simple solvation model showing the individual terms contributing to conformational free energies (where solvophobic effects are negligible). E_{O} and E_{H} correspond to the intramolecular steric and electronic effects in the O- and H-conformers respectively, and α_{S} , α_{O} , α_{H} , β_{S} , β_{O} , and β_{H} are the global hydrogen-bond donor (α) and acceptor constants (β) of the solvent, and the O- and the H-conformers respectively.

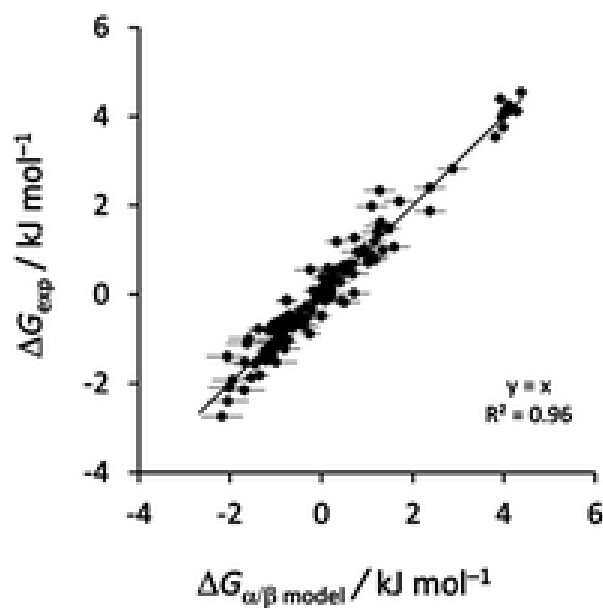


Figure 4. Correlation between experimentally determined conformational free energies (ΔG_{exp}) and corresponding values predicted from the α/β model for balances 1–11 in 13 different solvents.

		ΔE /kJ mol ⁻¹		$\Delta\alpha$		$\Delta\beta$	
1	<i>p</i> -NEt ₂	-2.8	± 0.4	0	± <0.1	+0.6	± 0.2
2	<i>p</i> -OMe	-1.6	± 0.2	0	± <0.1	+0.3	± 0.1
3	H	-1.2	± 0.2	0	± <0.1	+0.1	± <0.1
4	<i>p</i> -Ph	-0.8	± 0.1	0	± <0.1	0	± <0.1
5	<i>p</i> -Br	+0.5	± 0.1	0	± <0.1	-0.2	± <0.1
6	<i>p</i> -CN	+1.9	± 0.4	-0.2	± <0.1	-0.4	± 0.3
7	<i>p</i> -NO ₂	+2.6	± 0.5	-0.2	± <0.1	-0.5	± 0.2
8	<i>o</i> -OMe	-2.3	± 0.3	+0.1	± <0.1	+0.8	± 0.3
9	<i>o</i> -Me	-2.1	± 0.4	+0.2	± <0.1	+0.8	± 0.2
10	di <i>o</i> -Me	-2.0	± 0.5	+0.3	± <0.1	+1.0	± 0.3
11	<i>o</i> -NO ₂	+3.6	± 0.3	+0.1	± <0.1	+0.2	± 0.1

Table 1. ΔE , $\Delta\alpha$ and $\Delta\beta$ determined for balances 1 – 11 by fitting experimental conformational free energies to the model shown in Figure 3.

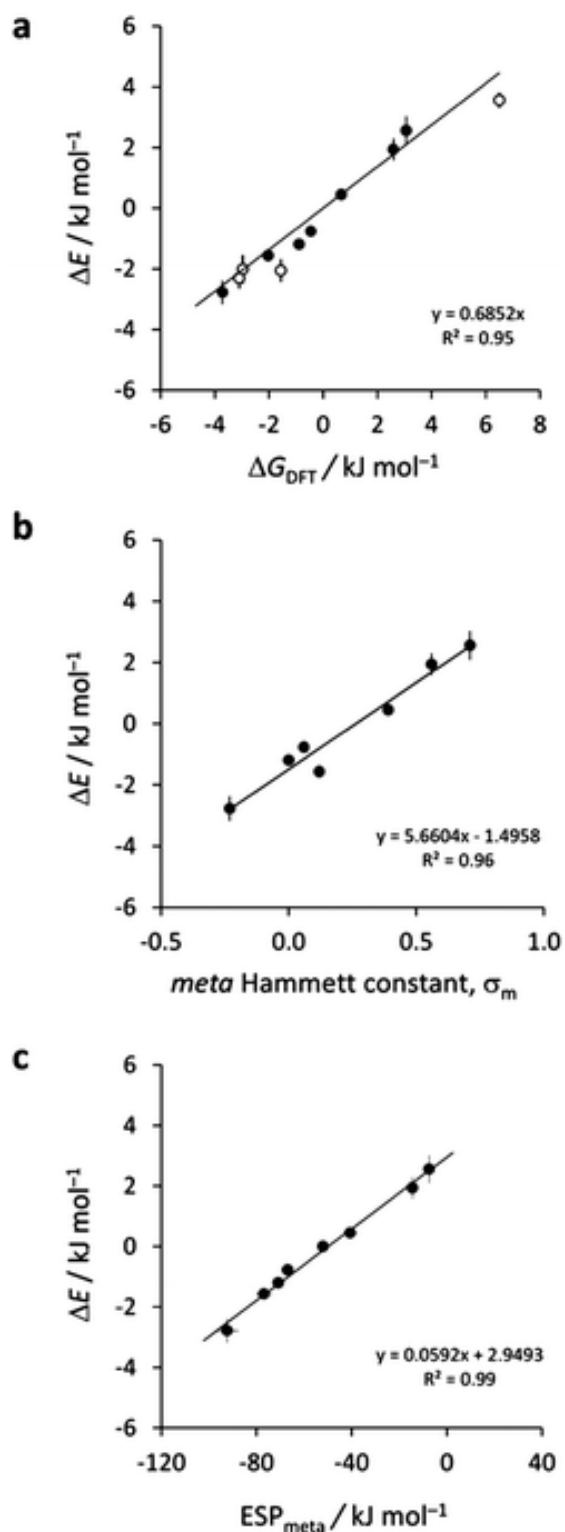


Figure 5. Correlation between the solvent-independent ΔE term dissected using the model in Fig. 3 and (a) gas-phase conformational free energies ΔG_{DFT} calculated using B3LYP/6-31G*, (b) meta Hammett substituent constants for the para-X substituents and, (c) the electrostatic potentials on the molecular surface over the carbon atoms positioned meta to the para X-substituent calculated using B3LYP/6-31G*. Data for the para-substituted balances 1–7 are indicated with black circles, and the ortho-substituted balances 8–11 by hollow circles, and is provided in Table S4.

Furthermore, the calculated electrostatic potential minima of these oxygen atoms correlate well with $\Delta\beta$ values determined for all 11 molecular balances in the O- and H-conformers (Figure 6). Looking beyond the major trends, closer examination of the $\Delta\alpha$ and $\Delta\beta$ terms provides an explanation for the more unusual experimental observations outlined in points i) to iii) above. In point i), it was noted that the *p*-EWG balances displayed a preference for the H-conformer as solvent polarity increased, while this behaviour was not observed in the *p*-EDG balances. This solvent-dependent switching of conformers whilst the substituent remains constant indicates that solvent effects in the most polar solvents must dominate over intramolecular interactions.

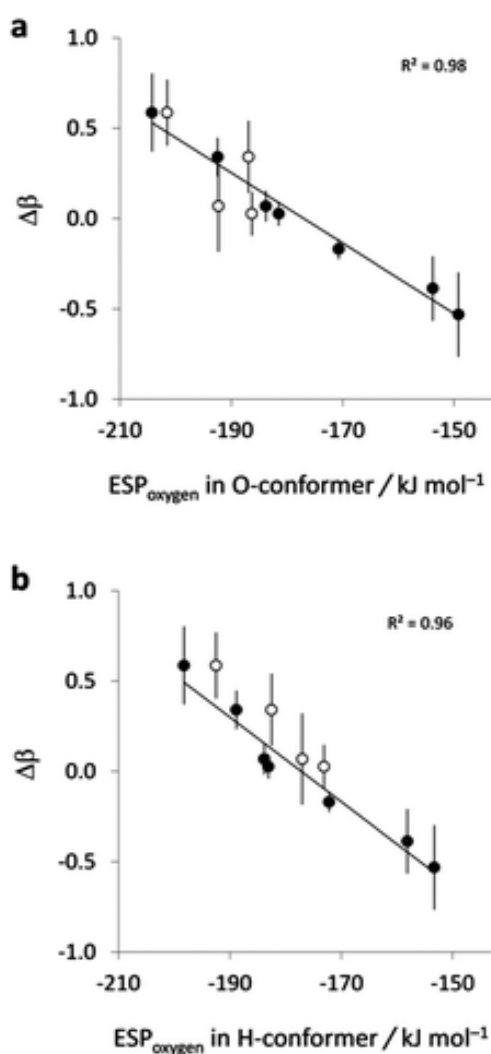


Figure 6. (a) Correlation between the $\Delta\beta$ term dissected using the model in Fig. 3 and the electrostatic potential minima over the formyl oxygen for balances 1–11 in the O- and H-conformers. Electrostatic potentials were calculated using B3LYP/6-31G*. The para-substituted balances 1–7 are indicated with black circles, and the ortho-substituted balances 8–11 by hollow circles. The corresponding data is provided in Table S5.

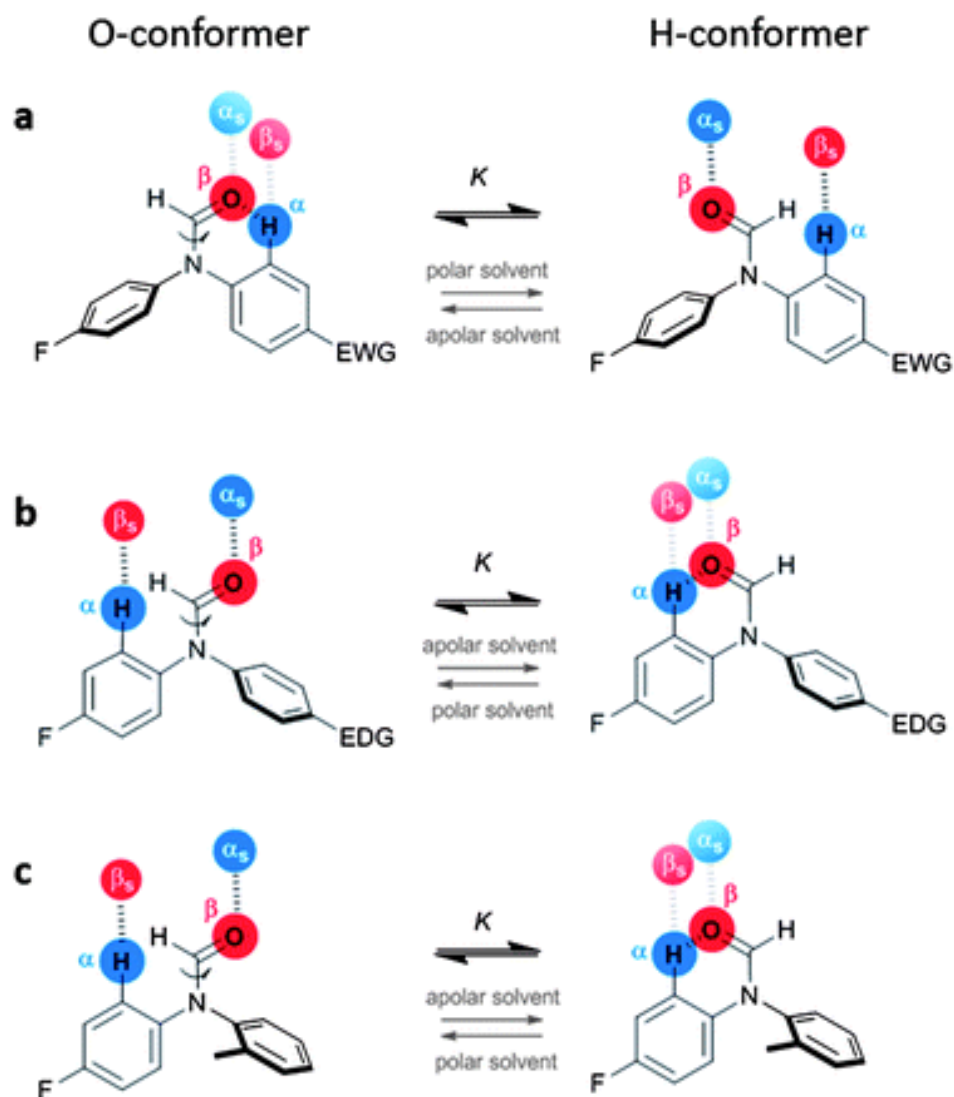


Figure 7. Proposed intramolecular and solvent interactions contributing to the conformational free energy differences in balances **1** to **11**. EDG = electron-donating group, EWG = electron-withdrawing group.

Taking the example of balance **7**, where $X = \text{NO}_2$; fitting the experimental data to the model depicted in Figure 3 gave $\Delta E = +2.6 \text{ kJ mol}^{-1}$, $\Delta\beta = -0.5$ and $\Delta\alpha = -0.2$. These solvent-dependent $\Delta\beta$ and $\Delta\alpha$ values are consistent with a possible role for solvent interactions competing with intramolecular interactions between the formyl oxygen and the protons on the edges of the aromatic rings. Although NMR data indicate that the *para*-substituted aromatic rings are freely rotating in solution, the average conformation of the rings may vary as the substituents are varied such that interactions between the formyl oxygen and the aromatic protons may influence the position of the conformational equilibrium

(in addition to the differences in the electrostatic potentials of the faces of the aromatic rings).

Support for this hypothesis can be found in the minimised calculated structures of these balances (Figures S5-S11, and the dihedral angles listed in Table S6, and shown in Figure 8), and crystal structures of related compounds (Figure S12), which show that aromatic rings bearing EWGs lie closer to the plane of the adjacent amide group, whilst rings bearing EDGs are twisted further from the plane of the amide. Rings bearing electron-withdrawing X-substituents could be expected to favour a more planar average conformation that allows conjugation between the EWG and the lone pair electrons of the formamide nitrogen, particularly when the proposed intramolecular interaction between the formyl oxygen and the edge of the polar aromatic can occur.

Evidence for intramolecular interactions between the formyl oxygen and the edges of the aromatic rings is provided by experimental NMR data (Figure 8). In the balances featuring *p*-EWGs the chemical shift of the proton implicated as being involved in the intramolecular hydrogen-bond is up to 0.3 ppm higher in the O-conformer compared to the H-conformer, while the adjacent protons, which are not involved in hydrogen-bonding interactions change by less than 0.04 ppm (Figure 8a and Table S8). Meanwhile the chemical shift trend is reversed for the *p*-EDG balances indicating that in these cases a weak intramolecular hydrogen bond is formed in the H-conformer rather than the O-conformer (Figure 8b). These chemical shifts are small, but nonetheless significant and are consistent with the weak nature of these interactions and rapid rotation of the aromatic rings about the aromatic C-N bond.

It follows that solvents with a strong hydrogen-bond acceptor constant such as DMSO will compete with the formyl oxygen in the binding of the polar aromatic protons, driving the equilibrium towards the H-conformer ($\Delta\alpha$ and $\Delta\beta = -ve$, Figure 7a). In contrast, the formyl oxygen interaction with the edge of the fluorine-substituted ring will be more favourable than the equivalent interactions with a ring bearing an EDG. Thus, when X is an EDG a polar solvent competes most with the intramolecular interactions involving the F-substituted ring, driving the conformation towards the O-conformer rather than the H-conformer ($\Delta\beta > 0$, Figure 7b). However, because the edge of a fluorine-substituted ring is less polar than those where X = NO₂ or CN, then even solvation by DMSO is not sufficient to fully overcome the intramolecular interactions encoded by ΔE and the H-conformer is still marginally preferred ($\Delta\alpha \approx 0$, Figure 2).

With reference to point ii) above, the sensitivity of the *ortho*-Me, di *ortho*-Me and *ortho*-OMe balances to variation of the solvent can also be explained within the framework of solvent competing with intramolecular electrostatic interactions. Calculated minimised structures show that *ortho*-substituents twist the substituted ring out of the plane of the formamide (dihedral angles in Figures 8c-f, and Figures S5-S11). The twist of the *ortho*-substituted ring means that a formyl oxygen-aromatic

edge interaction can only be formed with the edge of the fluorine-substituted ring (Figure 7c). Accordingly, the chemical shifts of the proton *meta* to the fluorine are seen to shift 0.2-0.3 ppm on going from the O- to the H-conformer (Figure 8c-e). In contrast, chemical shifts on all protons on the *ortho*-X-substituted rings either change little between conformers (X = *o*-OMe and di *o*-Me, Figure 8c, 8e), or are shifted in the opposite direction to that consistent with formation of an internal hydrogen-bond in the H-conformer. Since such shifts are seen in both the *ortho* and *para* protons in the X = *o*-Me (and *o*-NO₂) balances, this can be attributed to a general decrease in the electron density of the X-substituted ring arising from removal of the electron-rich formyl oxygen from above the ring on going from the O- to the H-conformer (Figure 8d and 8f). Thus, according to the solvation model depicted in Figure 7c, even solvents that are weakly solvating are able to break the weak intramolecular interactions with the F-substituted ring and drive the balances towards the readily solvated O-conformer (in which even less intramolecular competition exists). This effect manifests itself in the positive $\Delta\alpha$ and $\Delta\beta$ terms listed in Table 1, which are significantly more positive than those encountered in *para*-series.

Finally, with regards to the relative insensitivity of the *o*-NO₂ balance to solvent effects (point iii) above), application of the solvent model shown in Figure 3 reveals $\Delta E = +3.6 \text{ kJ mol}^{-1}$, $\Delta\alpha = +0.1$ and $\Delta\beta = +0.1$, indicating that the strong preference for the O-conformer is driven almost entirely by intramolecular interactions. In contrast to the other *ortho*-substituted balances investigated, both NMR chemical shifts and minimised geometry calculations are consistent with a minimal influence of solvent-sensitive interactions between the formyl oxygen and the edges of either the F- or the *o*-NO₂ substituted rings (Figure 8f and Tables S7-S8). Instead, the minimised structure of the highly favoured O-conformation reveals that the oxygen of the formyl group is positioned above the δ -positive nitrogen atom and adjacent aromatic carbon (Figure 9). This contact may be the driving force for the strong preference for the O-conformer in solution and calculated in the gas-phase, and appears similar to other favourable oxygen-carbonyl interactions that have been previously reported.^{32-34, 40, 41} Notably, the dissected ΔE value is $+3.6 \pm 0.3 \text{ kJ mol}^{-1}$ (towards the O-conformer hosting the C=O \cdots NO₂ interaction), which is within error of the estimated strength of the C=O \cdots NO₂ interaction of -3.3 kJ mol^{-1} obtained by taking the average of the difference between ΔG_{exp} for the *p*-NO₂ and *o*-NO₂ balances in all of the solvents examined (to control for background electronic and solvent effects).

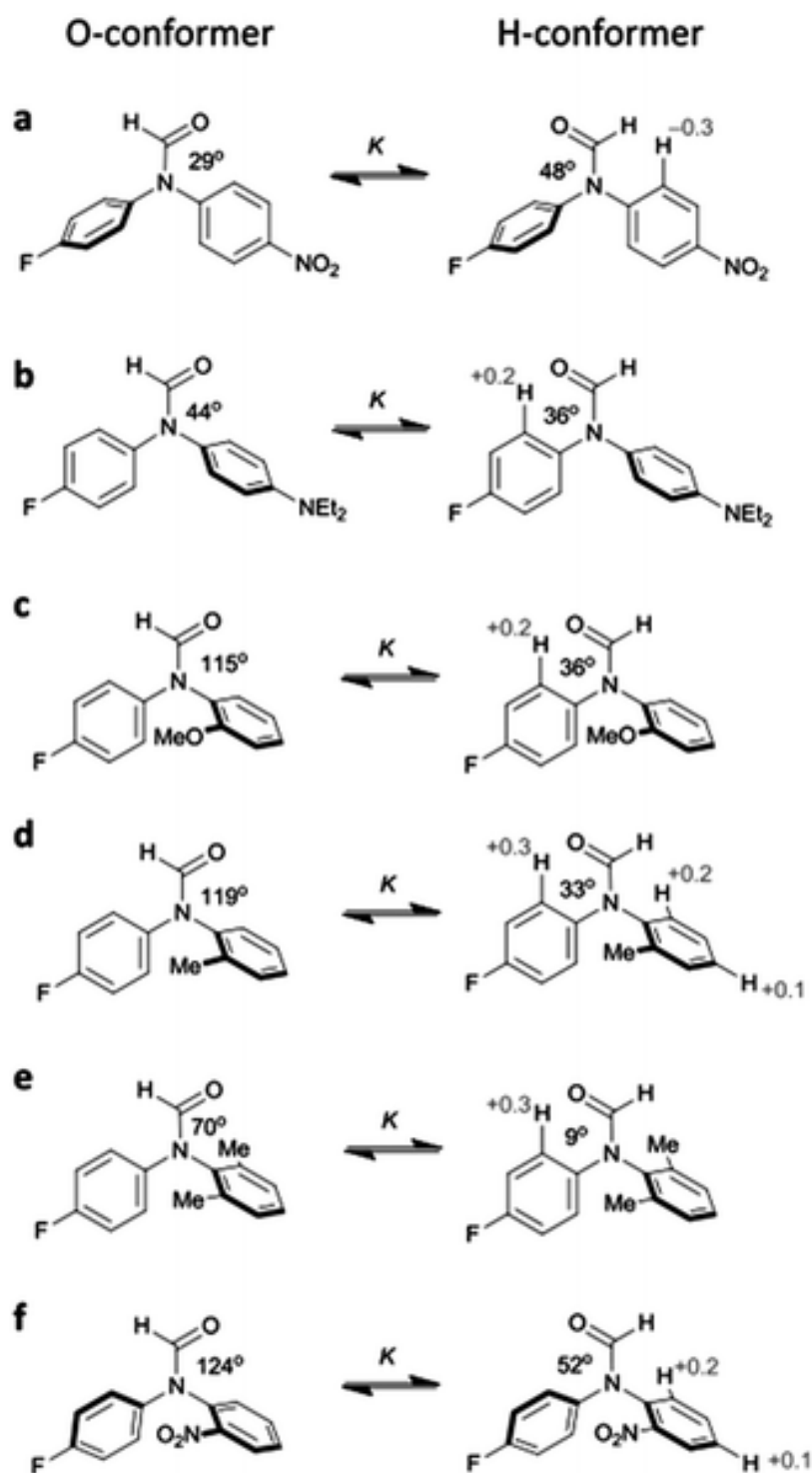


Figure 8. Experimental changes in proton chemical shift on going from the O-conformer to the H-conformer in CDCl_3 (grey text), and dihedral angles between the CH-aromatic plane and the formamide plane ($C_{\text{ortho}}-C_{\text{ipso}}-N_{\text{amide}}-C_{\text{amide}}$) from minimised conformer structures calculated using B3LYP/6-31G* (Figures S5-S11). Only chemical shifts greater than ± 0.1 ppm are shown, and a complete table of chemical shifts is provided in Tables S7-S8.

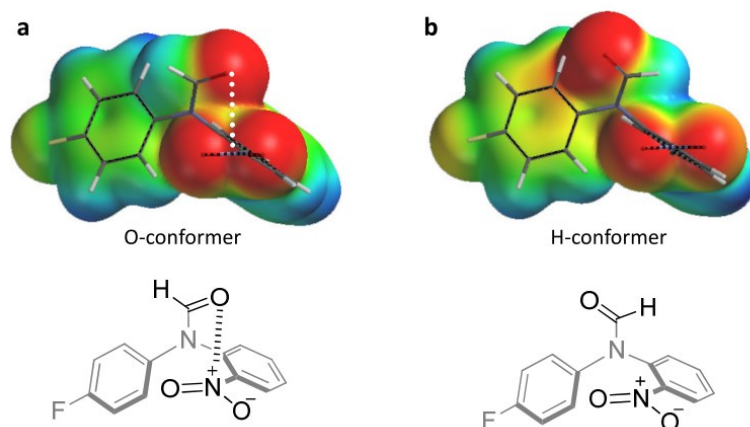


Figure 9. Electrostatic surface potentials and minimised geometries of the *ortho*-NO₂ balance (**11**) in the O- and H-conformations showing alignment and contact of the formamide oxygen with the δ -positive nitrogen of the nitro group. The structures and electrostatic potentials were calculated using B3LYP/6-31G*, and electrostatic potentials are scaled from -125 kJ mol^{-1} (red) to $+125 \text{ kJ mol}^{-1}$ (blue).

Conclusions

This study demonstrates how complicated behaviour may arise in seemingly simple chemical systems as a result of the interplay of conformational, intramolecular and solvent effects. Despite these complexities, the application of a simple solvation model was able to provide insight into the individual interactions governing the behaviour observed in 11 different molecular balances in 13 different solvents. The approach allowed the main energy contributions governing conformer populations to be dissected into three main constituents – an intramolecular component, ΔE , and solvent-dependent hydrogen-bond donor and acceptor components, $\Delta\alpha$ and $\Delta\beta$. The ΔE term was found to correlate with calculated free energy differences between conformers and to reveal intramolecular interactions that could be attributed mostly to the electronic effects of the substituents. The hypotheses describing the experimental trends were further supported by NMR chemical shift data and calculated electrostatic potentials. An unanticipated, yet strikingly favourable C=O \cdots NO₂ interaction was identified in one of the molecular balances investigated, which was determined to be driven almost entirely by direct intramolecular interactions and not by solvent effects. The approach may provide a useful platform testing theoretical models of solvation and for revealing the underlying principles influencing molecular recognition phenomena and the behaviour of other systems. It will be interesting to see the limitations of the simple method employed here, and whether more sophisticated solvation models⁴² will be better suited to tackling the challenges presented by larger chemical systems.

Notes and references

- [1] R. R. Knowles and E. N. Jacobsen, *Proc. Nat. Acad. Sci. USA*, 2010, 107, 20678-20685.
- [2] J. Meeuwissen and J. N. H. Reek, *Nat. Chem.*, 2010, 2, 615-621.
- [3] A. G. Doyle and E. N. Jacobsen, *Chem. Rev.*, 2007, 107, 5713-5743.
- [4] C. S. Chow and F. M. Bogdan, *Chem. Rev.*, 1997, 97, 1489-1514.
- [5] H.-J. Böhm and G. Klebe, *Angew. Chem. Int. Ed. Engl.*, 1996, 35, 2588-2614.
- [6] C. Bissantz, B. Kuhn and M. Stahl, *J. Med. Chem.*, 2010, 53, 5061-5084.
- [7] D. H. Williams, E. Stephens, D. P. O'Brien and M. Zhou, *Angew. Chem. Int. Ed.*, 2004, 43, 6596-6616.
- [8] E. T. Kool, *Chem. Rev.*, 1997, 97, 1473-1488.
- [9] D. W. Bolen and G. D. Rose, *Ann. Rev. Biochem.*, 2008, 77, 339-362.
- [10] D.-W. Zhang, X. Zhao, J.-L. Hou and Z.-T. Li, *Chem. Rev.*, 2012.
- [11] L. Brunsveld, B. J. B. Folmer, E. W. Meijer and R. P. Sijbesma, *Chem. Rev.*, 2001, 101, 4071-4098.
- [12] D. L. Cameron, J. Jakus, S. R. Pauleta, G. W. Pettigrew and A. Cooper, *J. Phys. Chem. B*, 2010, 114, 16228-16235.
- [13] J. L. Cook, C. A. Hunter, C. M. R. Low, A. Perez-Velasco and J. G. Vinter, *Angew. Chem. Int. Ed.*, 2007, 46, 3706-3709.
- [14] R. Cabot and C. A. Hunter, *Chem. Soc. Rev.*, 2012, 41, 3485-3492.
- [15] S. L. Cockroft and C. A. Hunter, *Chem. Commun.*, 2006, 3806-3808.
- [16] S. L. Cockroft and C. A. Hunter, *Chem. Commun.*, 2009, 3961-3963.
- [17] L. F. Newcomb and S. H. Gellman, *J. Am. Chem. Soc.*, 1994, 116, 4993-4994.
- [18] M. Ōki, *Acc. Chem. Res.*, 1990, 23, 351-356.
- [19] S. Paliwal, S. Geib and C. S. Wilcox, *J. Am. Chem. Soc.*, 1994, 116, 4497-4498.
- [20] E.-i. Kim, S. Paliwal and C. S. Wilcox, *J. Am. Chem. Soc.*, 1998, 120, 11192-11193.

- [21] I. K. Mati and S. L. Cockroft, *Chem. Soc. Rev.*, 2010, 39, 4195-4205.
- [22] K. B. Muchowska, C. Adam, I. K. Mati and S. L. Cockroft, *J. Am. Chem. Soc.*, 2013, 135, 9976-9979.
- [23] F. R. Fischer, W. B. Schweizer and F. Diederich, *Chem. Commun.*, 2008, 4031-4033.
- [24] A. E. Aliev, J. Moise, W. B. Motherwell, M. Nic, D. Courtier-Murias and D. A. Tocher, *Phys. Chem. Chem. Phys.*, 2009, 11, 97-100.
- [25] B. Bhayana and C. S. Wilcox, *Angew. Chem. Int. Ed.*, 2007, 46, 6833-6836.
- [26] W. R. Carroll, P. Pellechia and K. D. Shimizu, *Org. Lett.*, 2008, 10, 3547-3550.
- [27] B. W. Gung and J. C. Amicangelo, *J. Org. Chem.*, 2006, 71, 9261-9270.
- [28] B. W. Gung, X. Xue and Y. Zou, *J. Org. Chem.*, 2007, 72, 2469-2475.
- [29] F. Cozzi and J. S. Siegel, *Pure Appl. Chem.*, 1995, 67, 683-689.
- [30] R. Annunziata, M. Benaglia, F. Cozzi and A. Mazzanti, *Chem. Eur. J.*, 2009, 15, 4373-4381.
- [31] W. B. Motherwell, J. Moise, A. E. Aliev, M. Nic, S. J. Coles, P. N. Horton, M. B. Hursthouse, G. Chessari, C. A. Hunter and J. G. Vinter, *Angew. Chem. Int. Ed.*, 2007, 46, 7823-7826.
- [32] F. R. Fischer, P. A. Wood, F. H. Allen and F. Diederich, *Proc. Nat. Acad. Sci. USA*, 2008, 105, 17290-17294.
- [33] F. R. Fischer, W. B. Schweizer and F. Diederich, *Angew. Chem. Int. Ed.*, 2007, 46, 8270-8273.
- [34] F. Hof, D. M. Scofield, W. B. Schweizer and F. Diederich, *Angew. Chem. Int. Ed.*, 2004, 43, 5056-5059.
- [35] C. Zhao, R. M. Parrish, M. D. Smith, P. J. Pellechia, C. D. Sherrill and K. D. Shimizu, *J. Am. Chem. Soc.*, 2012, 134, 14306-14309.
- [36] C. A. Hunter, *Angew. Chem. Int. Ed.*, 2004, 43, 5310-5324.
- [37] C. A. Hunter and H. L. Anderson, *Angew. Chem. Int. Ed.*, 2009, 48, 7488-7499.
- [38] J. L. Cook, C. A. Hunter, C. M. R. Low, A. Perez-Velasco and J. G. Vinter, *Angew. Chem. Int. Ed.*, 2008, 47, 6275-6277.

- [39] The inclusion of a solvophobic term ($\Delta\alpha s\beta s$) did not significantly improve the quality of the fitting, consistent with the fact that the O- and H-conformers have very similar solvent-accessible areas (Figure S5-S11)
- [40] Z. Yin, L. Jiang, J. He and J.-P. Cheng, *Chem. Commun.*, 2003, 2326-2327.
- [41] K. J. Kamer, A. Choudhary and R. T. Raines, *J. Org. Chem.*, 2012, 78, 2099-2103.
- [42] C. A. Hunter, *Chem. Sci.*, 2013, 4, 1687-1700.